Supporting Information

Core-Corona Co/CoP Cluster Strung on Carbon Nanotubes as Schottky Catalyst for Glucose Oxidation Assisted H_2 production

Yuanyuan Zhang [a], Yunfeng Qiu*[a,b], Zhuo Ma [c], Yanping Wang, Yongxia Zhang [a], Yuxin Ying [d], Yinan Jiang [d], Yixue Zhu [d] and Shaoqin Liu*[a,b]

[a.] *School of Chemistry and Chemical Engineering, Harbin Institute of Technology, No.92 West Dazhi Street, Nan Gang District, Harbin, 150001, People's Republic of China.*

[b.] *Key Laboratory of Micro-systems and Micro-structures Manufacturing, Harbin Institute of Technology, No.2 Yikuang Street, Nan Gang District, Harbin 150080, People's Republic of China.*

[c.] *School of Life Science and Technology, Harbin Institute of Technology, No.92 West Dazhi Street, Nan Gang District, Harbin, 150001, People's Republic of China.*

[d.] *School of Materials Science and Engineering, Harbin Institute of Technology, Harbin, 150001, P.R. China.*

Email address: qiuyf@hit.edu.cn (Y.F. Qiu); shaoqinliu@hit.edu.cn (S.Q. Liu)

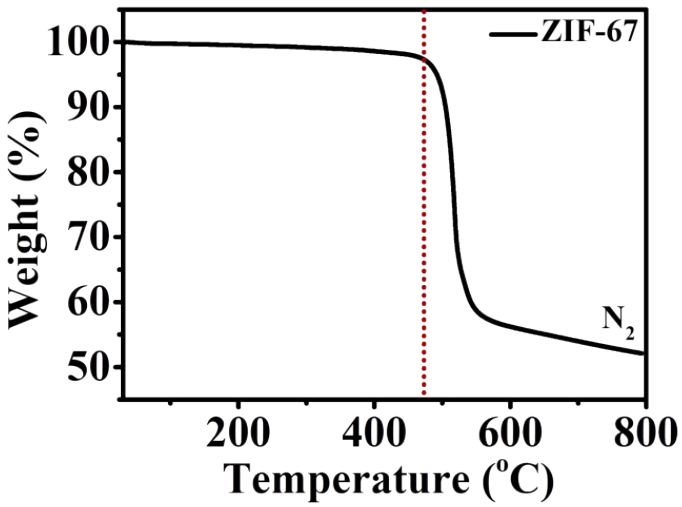

Figure S1. TGA curve for carbide of ZIF-67 in N_2.

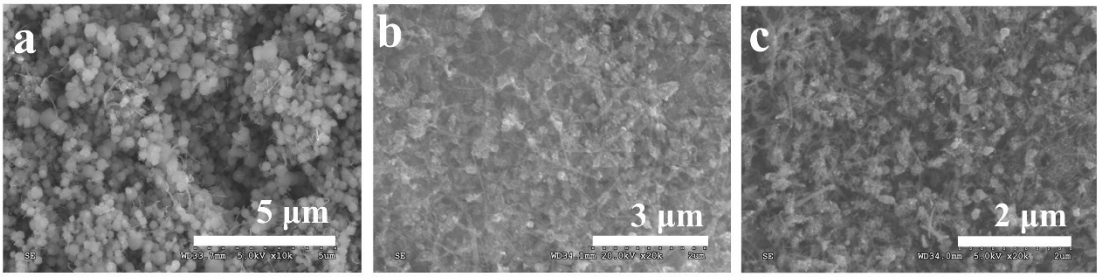

Figure S2. Analysis of morphologies. Low-resolution SEM images of (a) CNTs@ZIF-67, (b) CNTs@Co, and (c) CNTs@Co/CoP_{300mg}, respectively.

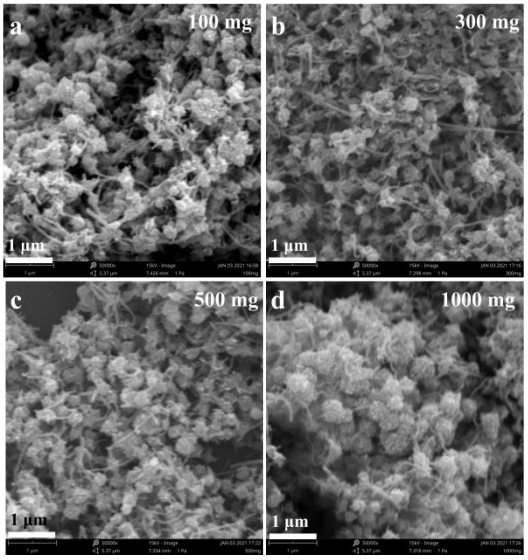

Figure S3. SEM images of CNTs@Co/CoP (a) 100, (b) 300, (c) 500 and (d) 1000 mg.

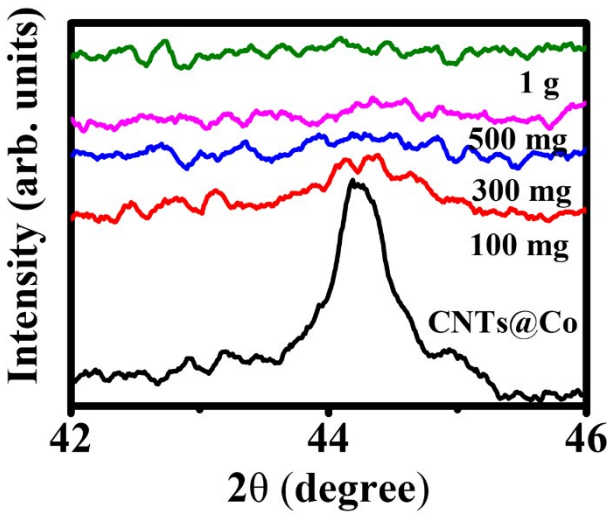

Figure S4. XRD patterns of CNTs@Co and CNTs@Co/CoP (100, 300, 500 and 1000 mg) in the 2θ range of 42 ~ 46°.

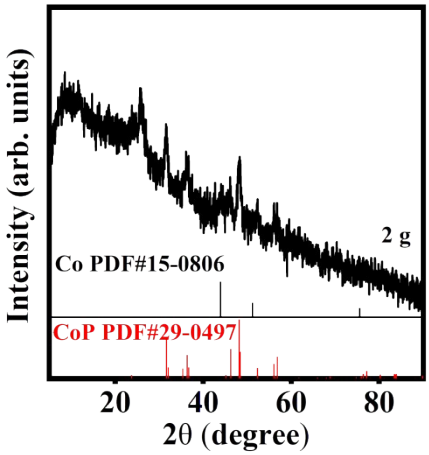

Figure S5. XRD pattern of CNTs@Co/CoP $_{2g}$ in the 2θ range of 5 ~ 90°.

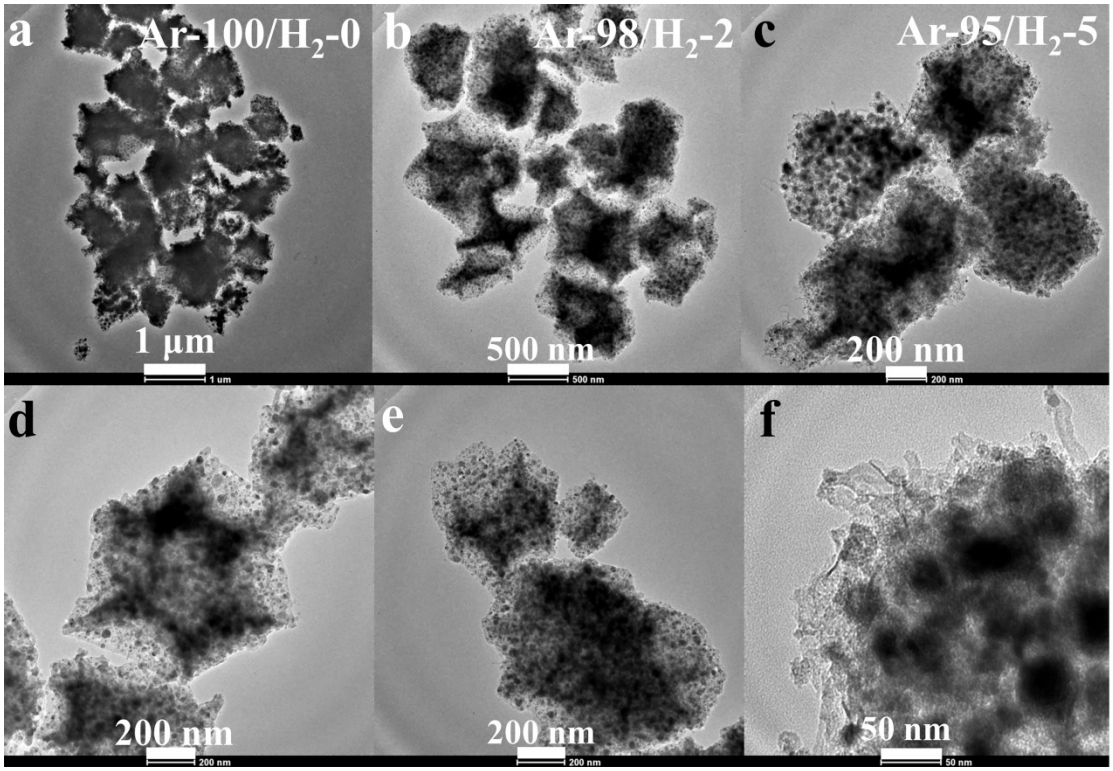

Figure S6. TEM images of ZIF-67 pyrolysis in different Ar/H_2 atmosphere. (a) Low-resolution and (d) high resolution TEM images of ZIF-67 pyrolysis in Ar/H_2 = 100:0 sccm. (b) Low-resolution and (e) high resolution TEM images of ZIF-67 pyrolysis in Ar/H_2 = 98:2 sccm. (c) Low-resolution and (f) high resolution TEM images of ZIF-67 pyrolysis in Ar/H_2 = 95:5 sccm.

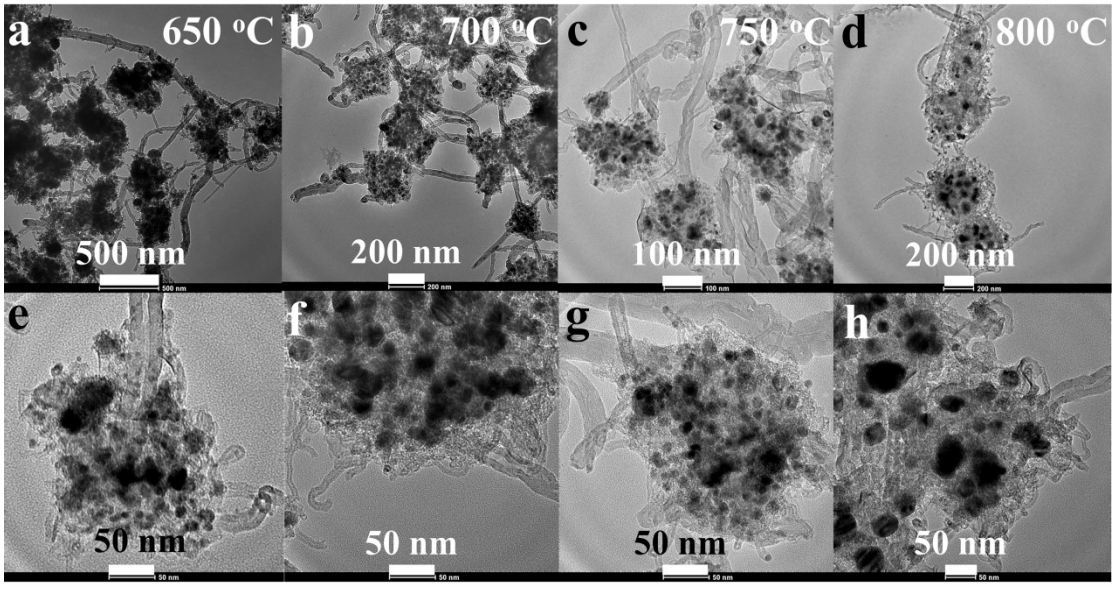

Figure S7. TEM images of CNTs@Co in different pyrolysis temperatures. (a) Low-resolution and (e) high resolution TEM images of 650 °C. (b) Low-resolution and (f) high resolution TEM images of 700 °C. (c) Low-resolution and (g) high resolution TEM images of 750 °C. (d) Low-resolution and (h) high resolution TEM images of 800 °C.

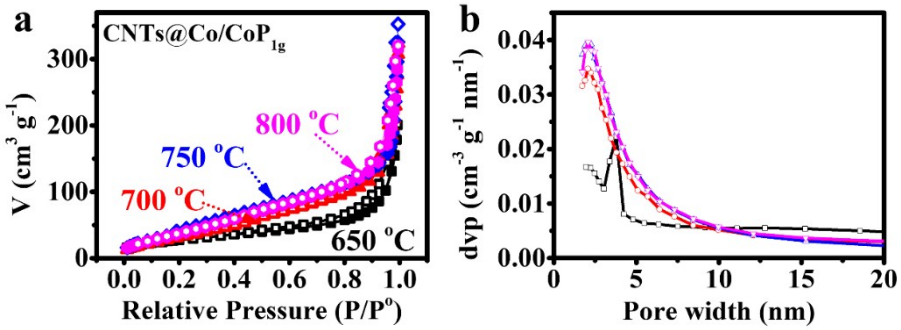

Figure S8. Pore size analysis. (a) Nitrogen adsorption-desorption isotherm, and (b) the corresponding pore size distribution of CNTs@Co/CoP_{1g} (T = 650 °C, 700 °C, 750 °C and 800 °C).

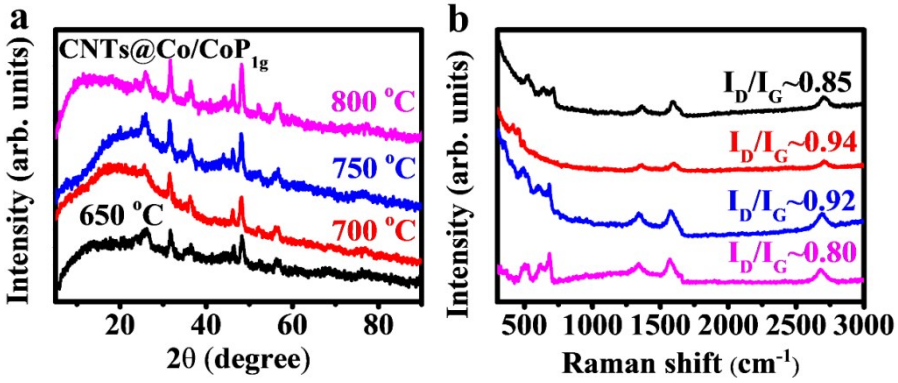

Figure S9. Characterization of material species and defect degree. (a) XRD patterns of CNTs@Co/CoP_T (1 g) (T = 650 °C, 700 °C, 750 °C and 800 °C) (b) Raman spectra of CNTs@Co/CoP_T (1 g) (T = 650 °C, 700 °C, 750 °C and 800 °C).

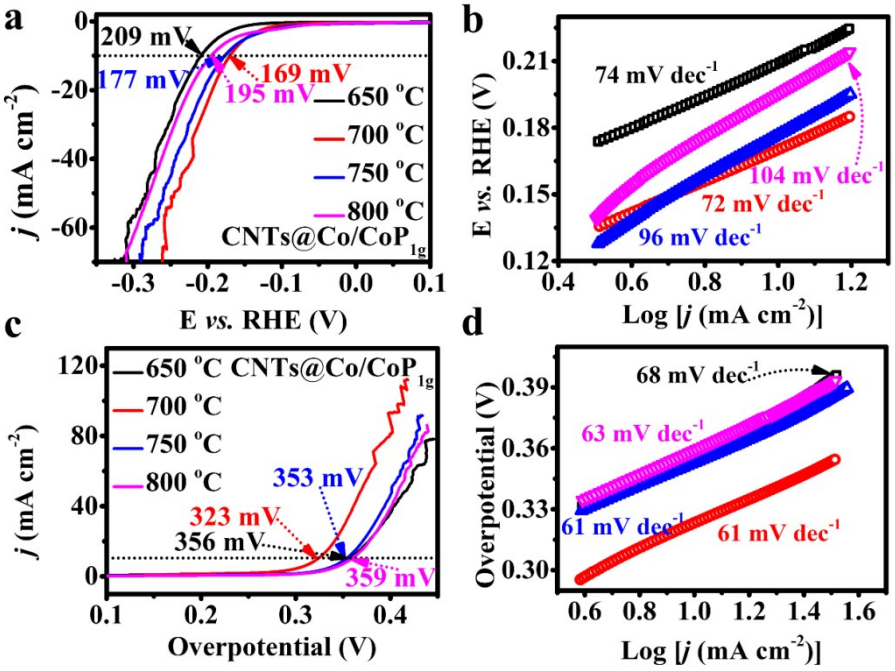

Figure S10. HER and OER measurements of CNTs@Co/CoP_T (1 g) (T = 650 °C, 700 °C, 750 °C and 800 °C) in 1.0 M KOH. (a, c) Polarization curves. All curves are recorded in N_2-saturated solution at a scan rate of 5 mV s^{-1}. (b, d) Corresponding Tafel curves.

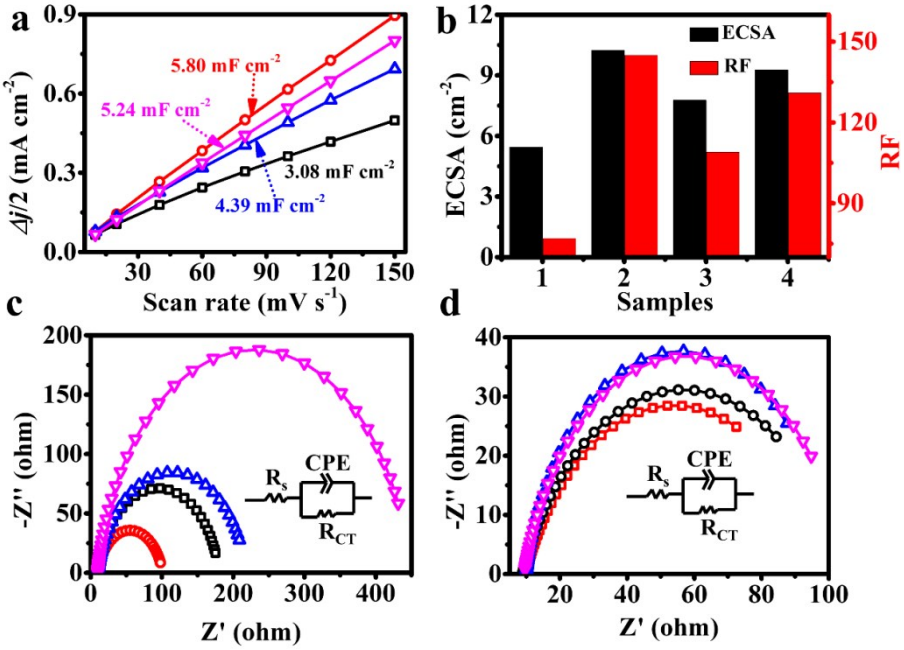

Figure S11. Cdl, ECSA, RF and R_{ct} analysis of CNTs@Co/CoP_T (1 g) (T = 650 °C, 700 °C, 750 °C and 800 °C). (a) Plots of Δj/2 vs. scan rates, (b) ECSA and RF for different catalysts and (c, d) Nyquist plots were measured at 169 mV and 323 mV in 1.0 m KOH electrolyte for HER and OER.

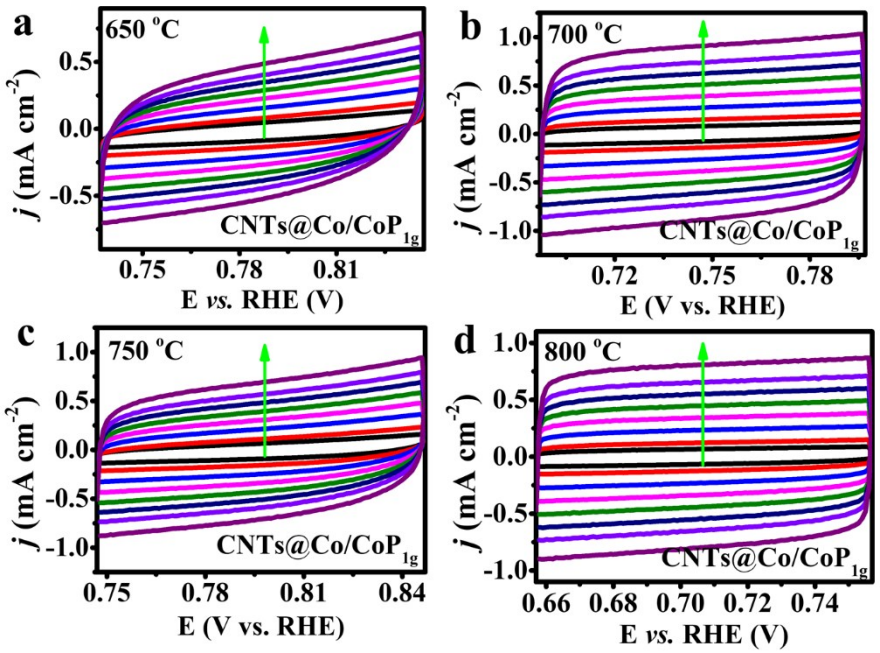

Figure S12. CV curves of CNTs@Co/CoP_T (1 g) at (a) 650 °C, (b) 700 °C, (c) 750 °C and (d) 800 °C, respectively.

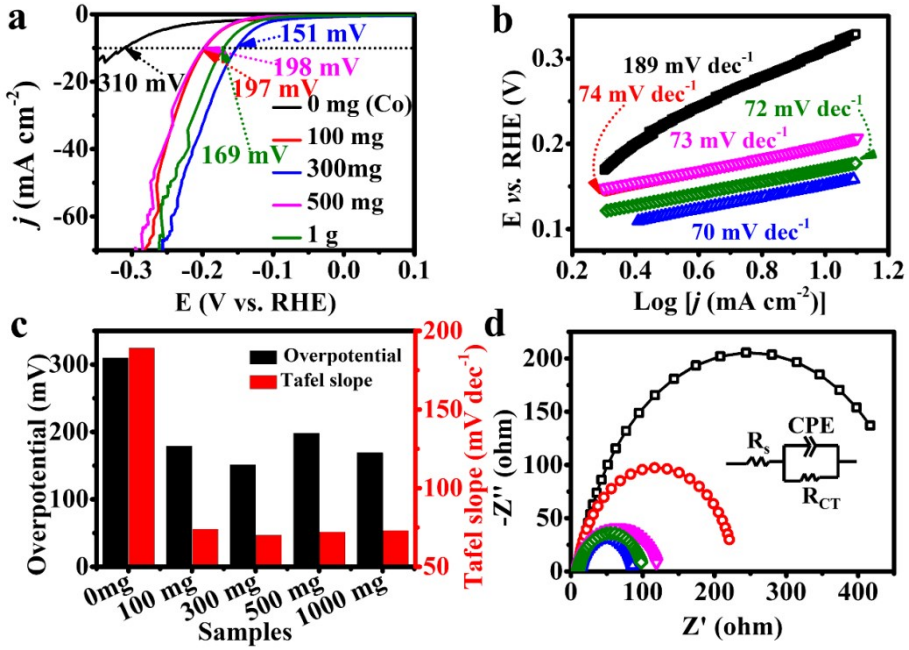

Figure S13. HER measurements of CNTs@Co and CNTs@Co/CoP (100 mg, 300 mg, 500 mg and 1 g). (a) Polarization curves. All curves are recorded in N_2-saturated 1 M KOH solution at a scan rate of 5 mV s^{-1}, (b) Corresponding Tafel curves, (c) Summary of overpotential at current density of 10 mA cm^{-2} and Tafel slopes, (d) Nyquist plots measured at -151 mV.

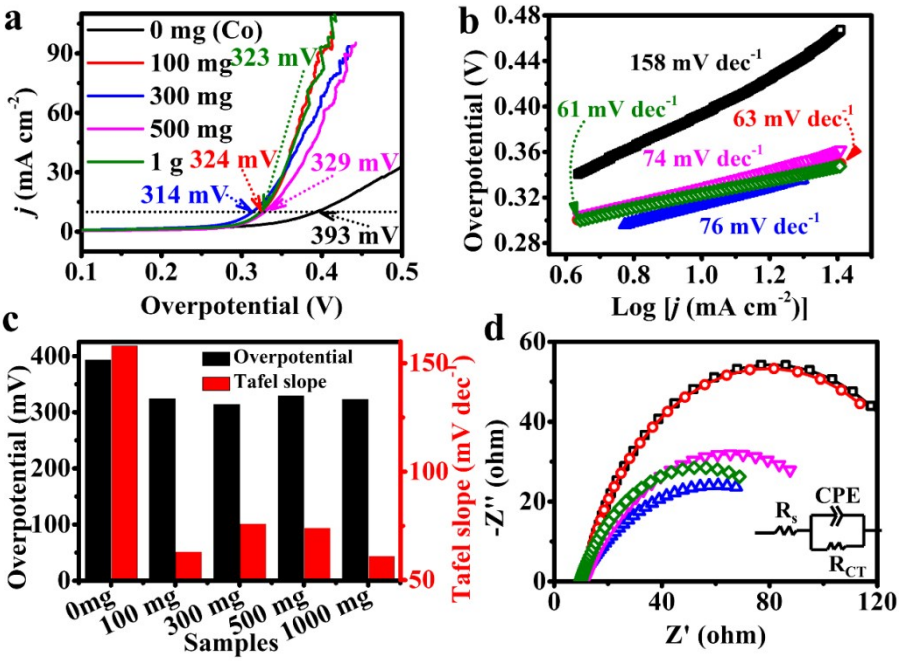

Figure S14. OER measurements of CNTs@Co and CNTs@Co/CoP (100 mg, 300 mg, 500 mg and 1 g). (a) Polarization curves. All curves are recorded in O_2-saturated 1 M KOH solution at a scan rate of 5 mV s^{-1}, (b) Corresponding Tafel curves, (c) Summary of overpotential at current density of 10 mA cm^{-2} and Tafel slopes, (d) Nyquist plots measured at 314 mV.

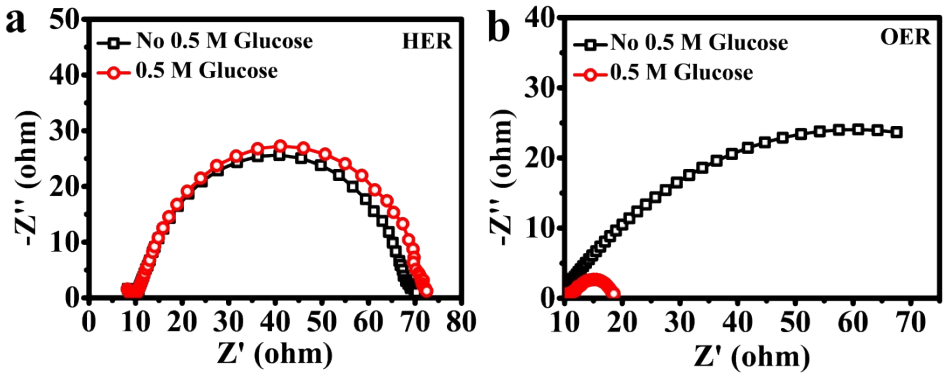

Figure S15. Nyquist plots with and without glucose of (a) HER and (b) OER.

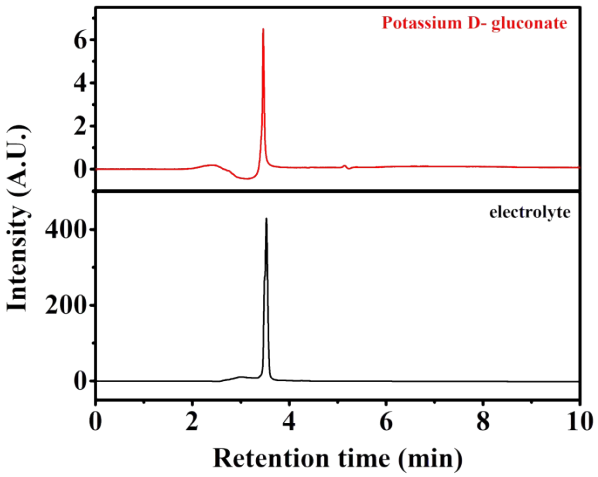

Figure S16. HPLC chromatograms for the electrolyte after GOR and standard solution (potassium D-gluconate).

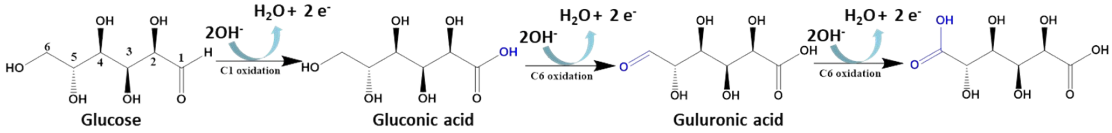

Figure S17. Schematic illustration of the possible pathway for the electrochemical oxidation of glucose to Gluconic acid (GNA) and Glucaric acid (GRA).

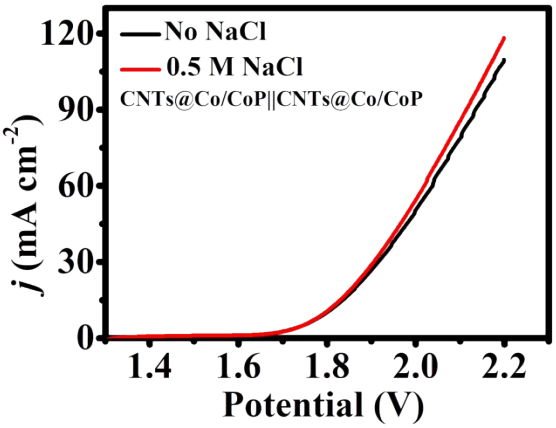

Figure S18. LSV curves of water electrolysis of CNTs@Co/CoP_{300mg}||CNTs@Co/CoP_{300mg} in 1M KOH solution without and with 0.5 M NaCl.

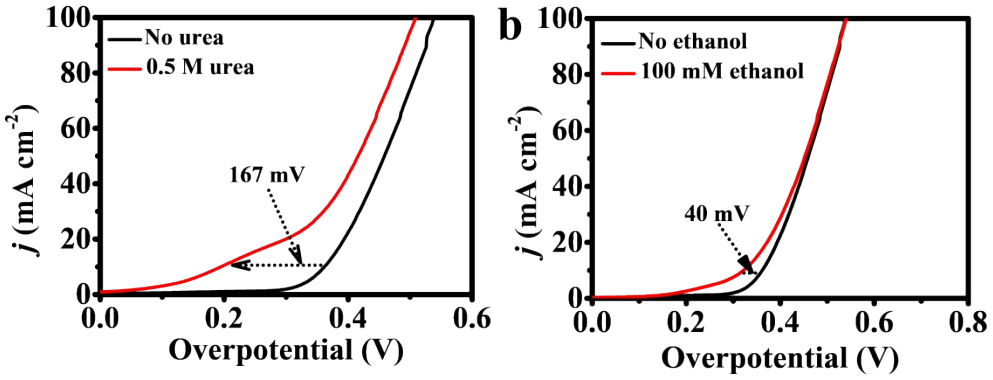

Figure S19. Polarization curves of OER measurements for CNTs@Co/CoP_{300mg} in 1 M KOH solution without and with (a) 0.5 M urea and (b) 100 mM ethanol.

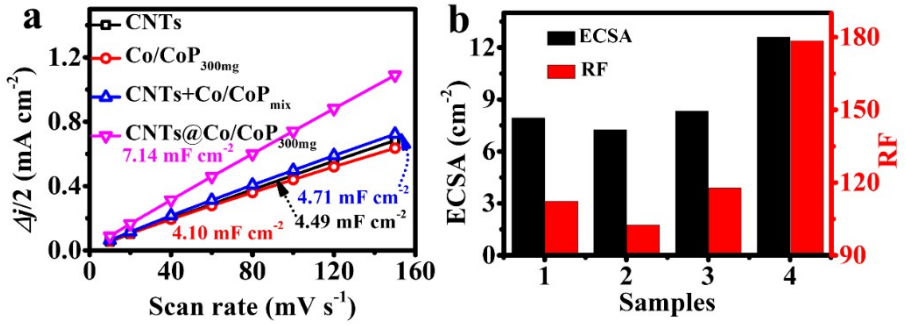

Figure S20. Cdl, ECSA and RF analysis of CNTs, Co/CoP, CNTs+Co/CoP_{mix}, CNTs@Co/CoP_{300mg}. (a) Plots of Δj/2 vs. scan rates, (b) ECSA and RF.

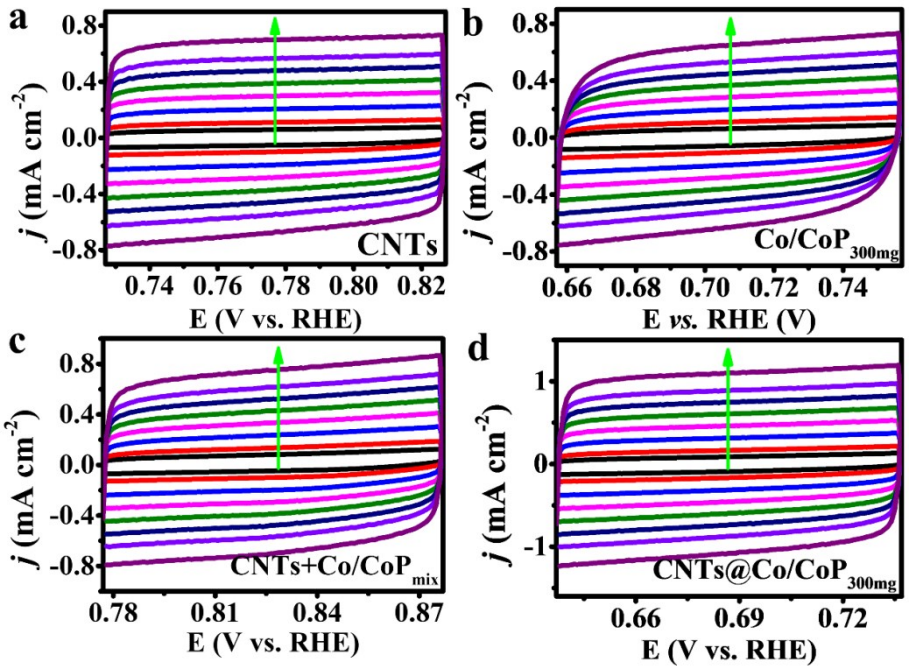

Figure S21. CV curves of (a) CNTs, (b) Co/CoP, (c) CNTs+Co/CoP_{mix}, (d) CNTs@Co/CoP_{300mg}, respectively.

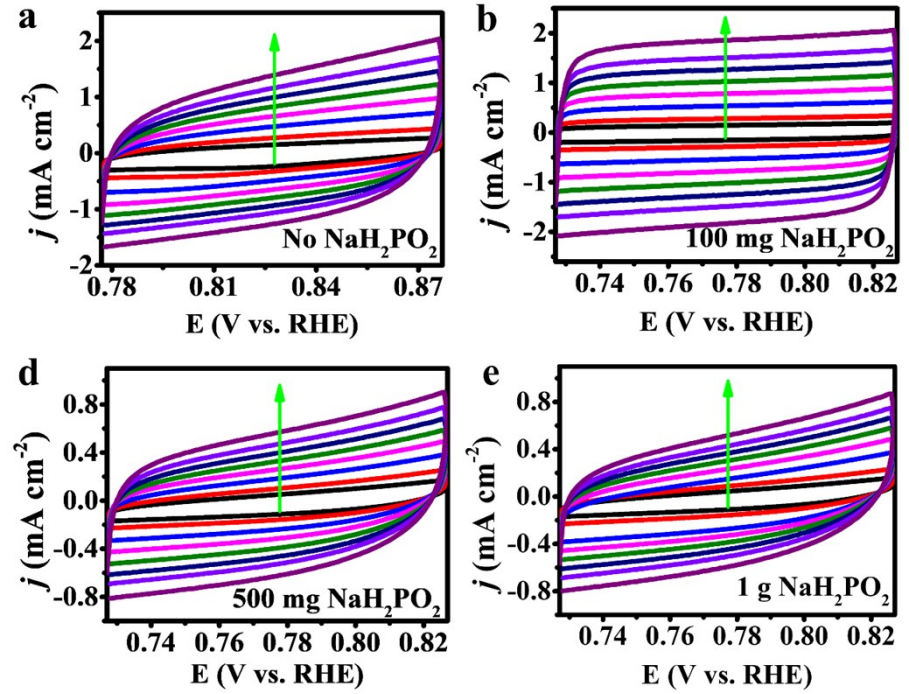

Figure S22. CV curves of (a) CNTs@Co, (b) CNTs@Co/CoP_{100mg}, (c) CNTs@Co/CoP_{500mg}, (d) CNTs@Co/CoP_{1g}, repectively.

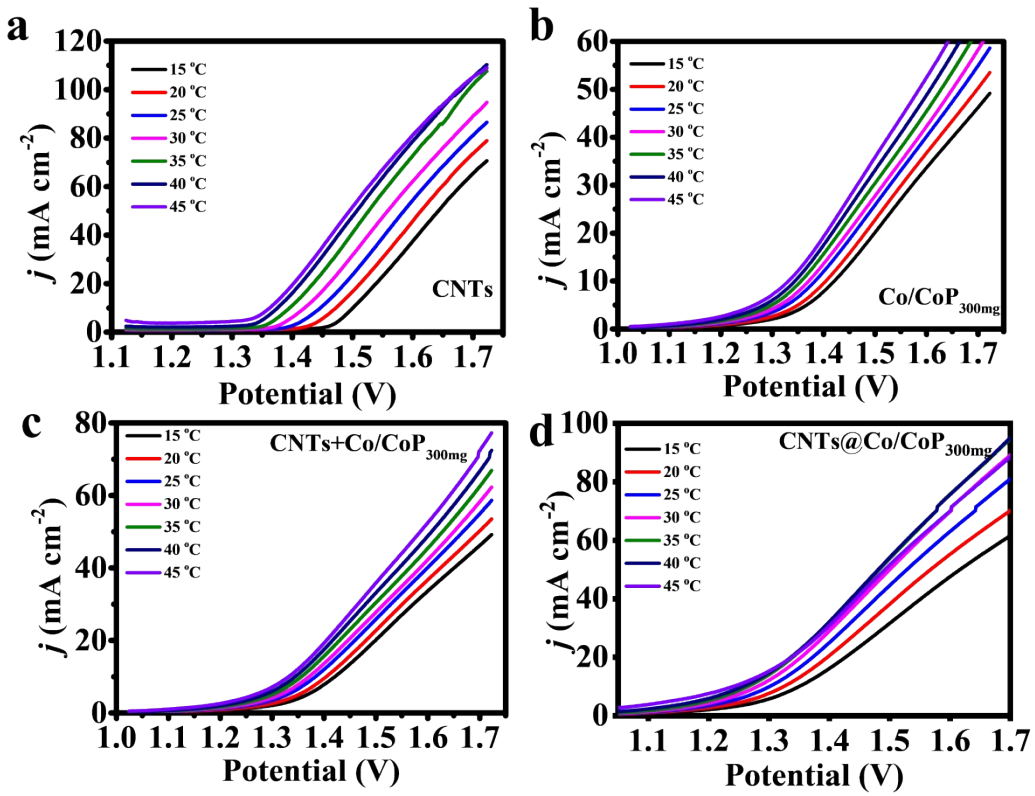

Figure S23. LSV curves of (a) CNTs, (b) Co/CoP_{300mg}, (c) $CNTs+Co/CoP_{300mg}$, and (d) $CNTs@Co/CoP_{300mg}$ in the electrolyte of 1 M KOH+0.5 M glucose at the temperature of 15°C, 20°C, 25°C, 30°C, 35°C, 40°C, and 45°C, respectively.

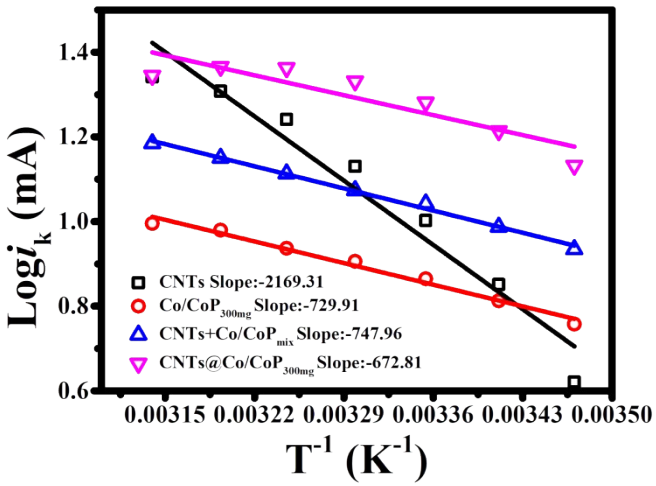

Figure S24. Log of the exchange current versus the inverse temperature for CNTs, Co/CoP_{300mg}, $CNTs+Co/CoP_{300mg}$, and $CNTs@Co/CoP_{300mg}$.

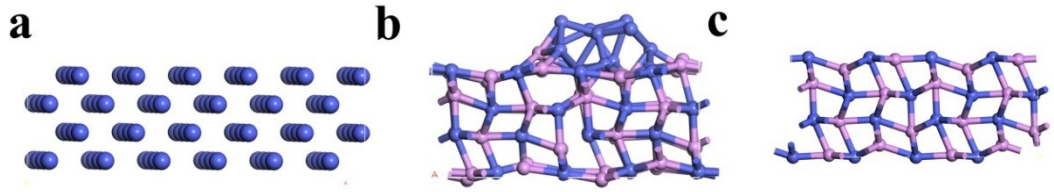

Figure S25. The crystal structure of (a) Co, (b) Co/CoP and (c) CoP.

Table S1. The average bader charge of Co in CoP and the average bader charge of Co layer.

Atom	bader charge transfer (e)
Co (CoP)	0.258
Co (Co)	-0.089
P	0.169

Table S2. Comparison of HER and OER performances of reported electrocatalyst in 1.0 M KOH for water splitting.

Catalysts		Eletrolyte (KOH)	Loading mass (mg cm^{-2})	J (mA cm^{-2})	η (mV vs RHE)	Tafel Slope (mV/dec)	Overall voltage (V)@10m A cm^{-2}	Ref
CoP/NCNHP	HER	1 M	2	-10	115	66	1.64	[1]
	OER			10	310	70		
Hollow Mo-CoP nanoarrays	HER	1 M	2.5	-10	40	65	1.56	[2]
	OER			10	305	56		
Carbon tubes/	HER	1 M	0.32	-10	190	131	1.743	[3]
cobalt-sulfide	OER			10	306	72		
CoP/GO-400	HER	1 M	0.28	-10	150	38	1.7	[4]
	OER			10	340	66		
CoP/PNC	HER	1 M	0.57	-10	165	70	1.68	[5]
	OER			10	300	77		
CoP@NPMG	HER	1 M	2.5	-10	150	75	1.58	[6]
	OER			10	276	54		
Mn-CoP	HER	1 M	-	-10	195	69	-	[7]
nanosheets	OER			10	290	76		
CoP/Co_2P	HER	1 M	0.36	-10	103	61.2	1.65	[8]
	OER			10	317	58.9		
NC-CNT/CoP	HER	1 M	1.5	-10	120	73	1.63	[9]
	OER			10	240	76		
Co/CoP	HER	1 M	0.22	-10	253	73.8	1.8	[10]
	OER			10	340	79.5		
$P\text{-}Co_3O_4$	HER	1 M	0.4	-10	120	52	1.76(η_{50})	[11]
	OER			10	280	69.8		
Ni_5P_4	HER	1 M	-	-10	150	53	1.7	[12]
	OER			10	290	40		
NiCoN-1H/CC	HER	1 M	-	-10	145	105.2	1.8(η_{13})	[13]
	OER			10	360	46.9		
$CoSe_2$ NS@CP	HER	1 M	0.16	-10	-	-	1.75	[14]
	OER			10	350	34.5		
$Fe_3O_4\text{-}CoP_x$	HER	1 M	-	-10	177	65	1.75	[15]
	OER			10	331	122		
$Co0_{.85}Se$@NC	HER	1 M	0.4	-10	230	125	1.76	[16]
	OER			10	32	75		
CNTs@CoP	HER	1 M	0.35	-10	169	70	1.74	This work
	OER			10	321	58		
SSUCo-900	HER	1 M	0.45	-10	247	86	1.88	[17]
	OER			10	337	-		

Table S3. Representative electrocatalytic hydrogen evolution coupled with organic oxidation reactions in aqueous media.

Catalyst	Electrolyte (KOH)	Organic substrate	η_{HER}(V) @10mA cm^{-2}	η_{OER} (V) @10mA cm^{-2}	$\eta_{OERorganic}$(V) @10mA cm^{-2}	Overall voltage (V) @10mA cm^{-2}	Overall voltage $_{organic}$ (V) @10mA cm^{-2}	Ref
S-MnO_2/NF	1 M	0.5 M urea	-	-	1.33	-	1.41	[18]
Ni_2P/NF	1 M	0.5 M Hydrazine	-0.29(η200)	-	0.018(η200)	1.6(η20)	1.0(η500)	[19]
Ni_2P NPA/NF	1 M	10 mM HMF	-0.15	1.5(onset)	1.35(onset)	1.65	1.44	[20]
Fe_2P/SSM	10 M	0.5 M glucose	-	1.43(onset)	1.33(onset)	1.52	1.22	[21]
CoP NWs/CC	1 M	40 mg L^{-1} Triclosan	-0.069	1.59	1.54	1.68	1.63	[22]
Fe11.1%-Ni_3S_2/NF	1 M	0.33 M urea	-0.126	1.482(η50)	-	1.60	1.46	[23]
hp-Ni	1 M	10 mM Benzyl alcohol	-0.219 (η50)	1.51	1.35	1.69	1.50	[24]
Ni_3N NA/CC	1 M	0.33 M urea	-0.136	1.57	1.35	1.56	1.44	[25]
CoS_2 NA/Ti	1 M	0.3 M urea	-0.14	-	1.4-1.5	1.63	1.59	[26]
NC@$CuCo_2N_x$/CF	1 M	15 mM Benzyl alcoho	-0.105	1.46	1.25	-	1.41	[27]
NiFeCo LDH/NF	1 M	0.33 M urea	-0.108	1.44	-	1.57	1.49	[28]
FQD/CoNi-LDH/NF	1 M	0.5 M urea	-0.15	1.57(η50)	1.36	1.59	1.45	[29]
MoS_2/Ni_3S_2/NiFe-LDH	1 M	0.5 M urea	- 0.261(η100)	1.544(η100)	1.396(η100)	1.559(η50)	1.343(η50)	[30]
Ni-Co_9S_8/CC	1 M	0.33 M urea	- 0.295(η100)	1.43	1.28	1.81	1.52	[31]
Co_x-$Ni(OH)_2$ NPs/CF	1 M	0.5 M urea	-0.106	1.56(η100)	1.3	1.73	1.37	[32]
CoMn/$CoMn_2O_4$	1 M	0.5 M urea	-0.069	1.61(η100)	1.36(η100)	1.64	1.51	[33]
CNTs@Co/CoP_{300m}	1 M	0.5 M glucose	-0.169	1.55	1.22	1.74	1.42	This work

References

1. Pan, Y.; Sun, K.; Liu, S.; Cao, X.; Wu, K.; Cheong, W.-C.; Chen, Z.; Wang, Y.; Li, Y.; Liu, Y.; Wang, D.; Peng, Q.; Chen, C.; Li, Y., *J. Am. Chem. Soc.* **2018,** *140* (7), 2610-2618.

2. Guan, C.; Xiao, W.; Wu, H.; Liu, X.; Zang, W.; Zhang, H.; Ding, J.; Feng, Y. P.; Pennycook, S. J.; Wang, J., *Nano Energy* **2018,** *48*, 73-80.

3. Zhang, X.; Wang, J.; Zhong, H.; Wang, Z.; Meng, F., *Acs Nano* **2016,** *10*, 2342-2348.

4. Jiao, L.; Zhou, Y.-X.; Jiang, H.-L., *Chem. Sci.* **2016,** *7* (3), 1690-1695.

5. Peng, Z.; Yu, Y.; Jiang, D.; Wu, Y.; Xia, B. Y.; Dong, Z., *Carbon* **2019,** *144*, 464-471.

6. Liu, Y.; Zhu, Y.; Shen, J.; Huang, J.; Yang, X.; Li, C., *Nanoscale* **2018,** *10* (5), 2603-2612.

7. Li, Y.; Jia, B.; Chen, B.; Liu, Q.; Cai, M.; Xue, Z.; Fan, Y.; Wang, H.-P.; Su, C.-Y.; Li, G., *Dalton T.* **2018,** *47* (41), 14679-14685.

8. Chen, L.; Zhang, Y.; Wang, H.; Wang, Y.; Li, D.; Duan, C., *Nanoscale* **2018,** *10* (45), 21019-21024.

9. Guan, C.; Wu, H.; Ren, W.; Yang, C.; Liu, X.; Ouyang, X.; Song, Z.; Zhang, Y.; Pennycook, S. J.; Cheng, C.; Wang, J., *J. Mater. Chem. A* **2018,** *6* (19), 9009-9018.

10. Xue, Z.-H.; Su, H.; Yu, Q.-Y.; Zhang, B.; Wang, H.-H.; Li, X.-H.; Chen, J.-S., *Adv. Energy Mater.* **2017,** *7* (12), 1602355.

11. Xiao, Z.; Wang, Y.; Huang, Y.-C.; Wei, Z.; Dong, C.-L.; Ma, J.; Shen, S.; Li, Y.; Wang, S., *Energ. Environ. Sci.* **2017,** *10* (12), 2563-2569.

12. Ledendecker, M.; Krick Calderón, S.; Papp, C.; Steinrück, H.-P.; Antonietti, M.; Shalom, M., *Angew. Chem. Int. Ed.* **2015,** *54* (42), 12361-12365.

13. Han, L.; Feng, K.; Chen, Z., *Energy Technol.* **2017,** *5* (11), 1908-1911.

14. Zhou, Y.; Xiao, H.; Zhang, S.; Li, Y.; Wang, S.; Wang, Z.; An, C.; Zhang, J., *Electrochim. Acta* **2017,** *241*, 106-115.

15. Guo, B.; Sun, J.; Hu, X.; Wang, Y.; Sun, Y.; Hu, R.; Yu, L.; Zhao, H.; Zhu, J., *ACS Appl. Nano Mater.* **2019,** *2* (1), 40-47.

16. Meng, T.; Qin, J.; Wang, S.; Zhao, D.; Mao, B.; Cao, M., *J. Mater. Chem. A* **2017,** *5* (15), 7001-7014.

17. Zhang, G.; Wang, P.; Lu, W.-T.; Wang, C.-Y.; Li, Y.-K.; Ding, C.; Gu, J.; Zheng, X.-S.; Cao, F.-F., *ACS Appl. Mater. Inter.* **2017,** *9* (34), 28566-28576.

18. Chen, S.; Duan, J.; Vasileff, A.; Qiao, S. Z., *Angew. Chem. Int. Ed.* **2016,** *55* (11), 3804-3808.

19. Tang, C.; Zhang, R.; Lu, W.; Wang, Z.; Liu, D.; Hao, S.; Du, G.; Asiri, A. M.; Sun, X.,

Angew. Chem. Int. Ed. **2017,** *56* (3), 842-846.

20. You, B.; Jiang, N.; Liu, X.; Sun, Y., *Angew. Chem. Int. Ed.* **2016,** *55* (34), 9913-9917.

21. Du, P.; Zhang, J.; Liu, Y.; Huang, M., *Electrochem. Commun.* **2017,** *83*, 11-15.

22. Lyu, C.; Zheng, J.; Zhang, R.; Zou, R.; Liu, B.; Zhou, W., *Mater. Chem. Front.* **2018,** *2* (2), 323-330.

23. Zhu, W.; Yue, Z.; Zhang, W.; Hu, N.; Luo, Z.; Ren, M.; Xu, Z.; Wei, Z.; Suo, Y.; Wang, J., *J.Mater. Chem. A* **2018,** *6* (10), 4346-4353.

24. You, B.; Liu, X.; Liu, X.; Sun, Y., *ACS Catal.* **2017,** *7* (7), 4564-4570.

25. Liu, Q.; Xie, L.; Qu, F.; Liu, Z.; Du, G.; Asiri, A. M.; Sun, X., *Inorg. Chem. Front.* **2017,** *4* (7), 1120-1124.

26. Wei, S.; Wang, X.; Wang, J.; Sun, X.; Cui, L.; Yang, W.; Zheng, Y.; Liu, J., *Electrochim. Acta* **2017,** *246*, 776-782.

27. Zheng, J.; Chen, X.; Zhong, X.; Li, S.; Liu, T.; Zhuang, G.; Li, X.; Deng, S.; Mei, D.; Wang, J.-G., *Adv. Funct. Mater.* **2017,** *27* (46), 1704169.

28. Babar, P.; Lokhande, A.; Karade, V.; Pawar, B.; Gang, M. G.; Pawar, S.; Kim, J. H., *ACS Sustain. Chem. Eng.* **2019,** *7* (11), 10035-10043.

29. Feng, Y.; Wang, X.; Huang, J.; Dong, P.; Ji, J.; Li, J.; Cao, L.; Feng, L.; Jin, P.; Wang, C., *Chem. Eng. J.* **2020,** *390*, 124525.

30. He, M.; Hu, S.; Feng, C.; Wu, H.; Liu, H.; Mei, H., *Int. J. Hydrog. Energy* **2020,** *45* (1), 23-35.

31. Hao, P.; Zhu, W.; Li, L.; Tian, J.; Xie, J.; Lei, F.; Cui, G.; Zhang, Y.; Tang, B., *Electrochim. Acta* **2020,** *338*, 135883.

32. Sun, C. B.; Guo, M. W.; Siwal, S. S.; Zhang, Q. B., *J. Catal.* **2020,** *381*, 454-461.

33. Wang, C.; Lu, H.; Mao, Z.; Yan, C.; Shen, G.; Wang, X., *Adv. Funct. Mater.* **2020,** *30* (21), 2000556.